2014 23rd International Lightning Detection Conference
18 - 19 March • Tucson, Arizona, USA
5th International Lightning Meteorology Conference
20 - 21 March • Tucson, Arizona, USA

Polarimetric radar analysis of lightning in an MCC event on June 15, 2013

Kun-Yuan Lee and Matthew S. Van Den Broeke

Department of Earth and Atmospheric Sciences
University of Nebraska-Lincoln
Lincoln, Nebraska

ABSTRACT

On June 15, 2013, a mesoscale convective complex (MCC) developed over northeast Oklahoma and tracked to southwest Illinois. This MCC brought damaging winds and heavy rain to the area, including thunderstorm wind gusts to 75 mph, resulting in a loss of power. Although many studies have investigated MCC events, they have rarely compared lightning structure with polarimetric radar variables. We will analyze the MCC using dimensional and locational analysis of the storm structure and locations of lightning relative to different MCC stages. We will also examine relationships between radar variables and lightning occurrence, to infer microphysical processes which may favor electric charge separation leading to lightning. We will also present differences between areas of the MCC which had lower vs. higher flash density. These characteristics will be related to the polarimetric radar variables, benefiting meteorologists who forecast such events, and allowing a better picture of storm structure than satellite data or non-polarimetric radar can provide.

I. INTRODUCTION

Mesoscale Convective Complexes (MCCs) remain of great interest for meteorologists because they are responsible for much severe weather (intense rainfall, damaging winds, tornadoes, hail, flash floods and lightning). Compared to the broader class of mesoscale convective systems (MCSs), MCCs are relatively rare, representing less than 1% of all MCSs in the western tropical Pacific (Mapes and Houze 1993) and a slightly larger fraction in North America (Mohr 1996). MCCs typically develop in the late afternoon or evening as individual convective storms combine in the region, and attain maximum anvil size between midnight and sunrise. Cloud-to-ground lightning activity in an MCC was studied by Goodman et al. 1986, who found that lightning damage occurs with half of MCCs. There has been increasing attention studying the lightning characteristics of MCCs, but most of these studies have focused on the physical process of lightning related to storm structure. For example, Makowski et al. (2012) discussed total lightning characteristics associated with the cloud shield area of an MCS. Cloud-to-ground (CG) lightning activity in an MCS was studied by Rutledge et al. (1987), who found a correlation between the peak convective rainfall amount and peak negative CG flash rate, and also between the peak stratiform rainfall amount and peak positive CG flash rate. Relatively few studies have looked at polarimetric radar variables in association with the lightning characteristics in MCCs. Accordingly, our study surveyed the distribution of lightning associated with polarimetric variables (Z_{HH}, Z_{DR}, ρ_{hv}, K_{DP}) throughout the life cycle of an MCC, with implications for the microphysical processes associated with lightning initiation. We believe this work will help the forecasting meteorologist to utilize the polarimetric variables and possibly to predict regions with maximum lightning flash rate.

II. DATA AND METHODS

Polarimetric radar datasets are analyzed from Weather Surveillance Radar—1988 Doppler (WSR-88D) network radars, including the Springfield, Missouri, radar (KSGF), Kansas City/Pleasant Hill, Missouri, radar (KEAX) and the St. Louis, Missouri radar (KLSX). The lightning data was provided by the Earth Networks Total Lightning Network. It detects a broad frequency range extending from 1 Hz to 12 MHz that detects both in-cloud (IC) and CG lightning. Total lightning data (CG and IC) was available from 1730 UTC on June 15, 2013, until 0200 UTC on June 16, 2013. Radar data was displayed using the Weather and Climate Toolkit software, and lightning data was displayed using shape files convert from ArcGIS software. The focus of this study will be from 2000 UTC on 15 June 2013, when the MCC was in its development stage, though the mature stage analyzed at approximately 2140 UTC, and ending at 0100 UTC on 16 June 2013 when the MCC decreased in intensity. Vertical cross-sections were analyzed using GR2Analyst. Satellite data was obtained from the NCAR image archive. We will discuss the polarimetric radar variables associated with lightning characteristics. To ensure a good match between lightning data points and radar data for each time displayed, we only include lightning data from the first 3 minutes after each radar scan start time. Most radar analyses were completed using the lowest elevation angle (0.54 degrees). Potential data quality issues will be discussed relevant to interpretation of the polarimetric variables.

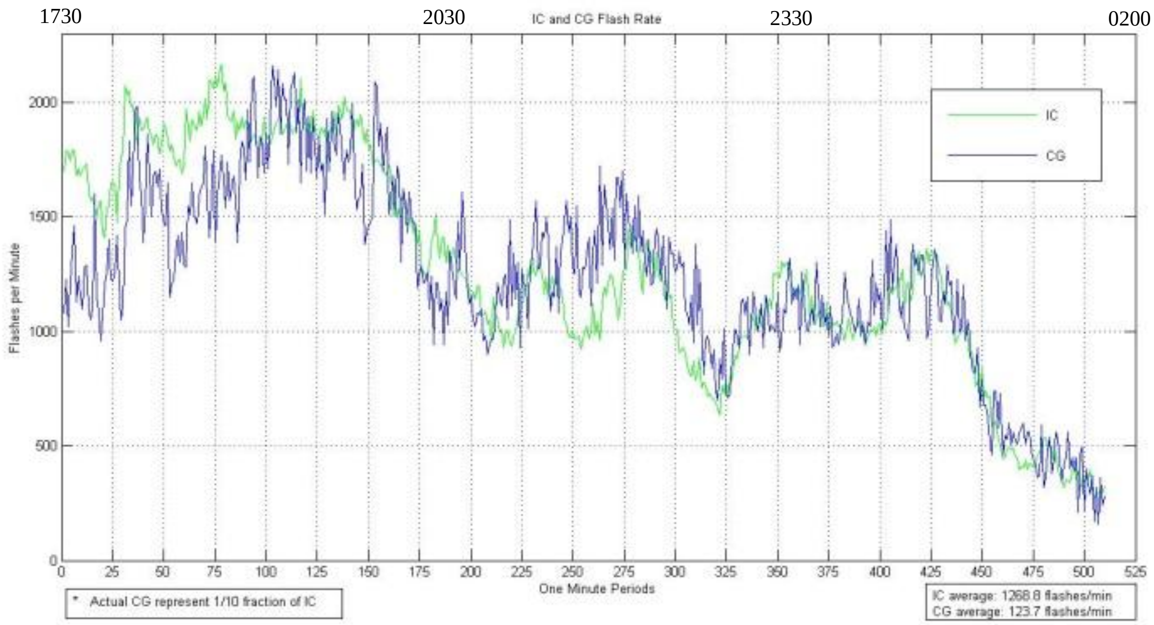

Figure.1 IC and CG flash rates from 0 (1730 UTC) to 515 (0200 UTC).

III. CLOUD-TO-GROUND AND IN-CLOUD LIGHTNING THROUGH THE MCC LIFE CYCLE

Relatively few studies have analyzed both CG and IC lightning distributions in MCCs. The lightning was analyzed for only a portion of the life cycle of most MCCs and the sampled portion of the life cycle varied, so most comparisons of flash characteristics among different systems should be viewed as preliminary. CG and IC lightning in the June 15, 2013, MCC had very different characteristics. IC lightning averaged about 1269 flashes per minute throughout the observed time (Fig. 1, 1730-0200 UTC), while CG lightning averaged about 124 flashes per minute. Prior work from Biggerstaff and Houze (1993), divided a typical MCS into convective and stratiform regions. Based on their categorization, the convective region has a very strong reflectivity gradient at the leading edge, and a large trailing stratiform precipitation region, often exhibiting a secondary maximum of reflectivity separated from the convective line by a narrow channel of lower reflectivity, called the transition zone. Maddox (1980) defined MCC life cycle stages of genesis, development, mature and dissipation. We divide the MCC into 3 parts and analyze 3 life cycle stages following these prior works: the convective region, the transition zone (behind the convective region) and the large trailing stratiform region (Fig. 2). Lightning analysis times were taken from the development, mature, and dissipation life cycle stages.

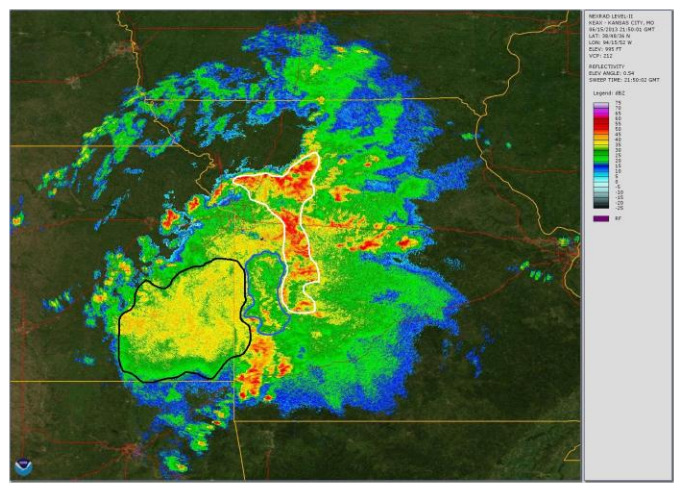

Figure.2 Area classification: convective area (white), transititon zone (blue), and trailing straifrom region (black) at 2018 UTC.

During the development stage of the MCC (observed from 2000-2020 UTC) most lightning strikes tended to occur near the region of high reflectivity (>50 dBZ), corresponding to deep convection in the convective region likely due to the presence of abundant ice crystals and mixed-phase particles in the vicinity of the convective region. CG lightning tended to cluster in the transition zone in areas of high reflectivity, while IC lightning was more uniformly spread through the high reflectivity region in both areas. The trailing stratiform region was located directly behind an electrically-active portion of the transition zone.

This region had little or no IC and CG lightning relative to the convective region and transition zone. The development stage of the MCC event had more lightning activity in the trailing stratiform region, possibly due to more individual convective cells merging into the MCC at this time. A prior study noted that occasionally, during the development stage of the MCC, flash initiations and reflectivity maxima in the trailing stratiform region appeared to be due to dissipating cells that had migrated from the convective line into the trailing stratiform region (Hunter et al. 1992). This finding agrees with what was observed in our trailing stratiform region, in which lightning strikes decreased when the MCC transitioned into the mature stage (Fig. 3).

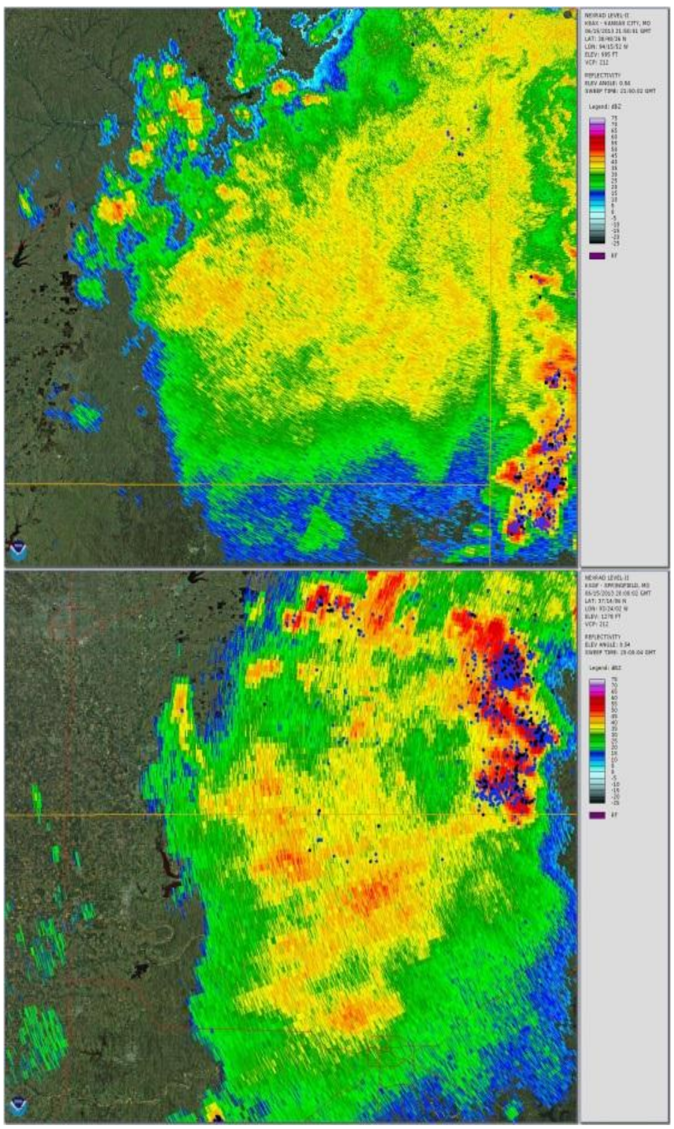

Figure 3. Comparison of lightning flash rates (black dots = CG, blue dots = IC) in trailing stratiform region in development stage (above; 2000 UTC) and mature stage (below; 2150 UTC).

In the mature stage of the MCC (observed from 2140-2200 UTC), the total lightning flash rate was very high within the high reflectivity regions along the northern boundary of the MCC and in a squall line southwest of the MCC. Lightning strikes decreased to near zero in the trailing stratiform region, but there were fewer lightning strikes located between the transition zone and convective cells which may be affected by sinking motion between cells.

In the dissipating stage of the MCC (observed from 0050-0110 UTC), the total lightning flash rate decreased dramatically, with remaining strikes concentrated in the high reflectivity regions associated with deep convection. IC lightning was located in the convective region and a portion of the transition zone, with very few strikes in the trailing stratiform region. IC and CG lightning located in the trailing stratiform region was comparably less than in the MCC's development and mature stages.

Both IC and CG lightning show little activity in the trailing stratiform region. Local convective cells with strong updraft and relatively high reflectivity within the MCC trailing stratiform region may also contain a higher flash rate. CG lightning tended to be widespread in both the convective region and transition zone, but the CG flash rate tended to be highest in the transition zone behind the strong updraft region (Fig. 10). The IC and CG lightning remain most active in the steep gradient of reflectivity in the dissipating stage, possibly due to the greater maturity of cells (high Z_{HH}) in this region. Both IC and CG decreased rapidly throughout the dissipating stage.

IV. LIGHTNING FLASH RATE ASSOCIATED WITH THE POLARIMETRIC RADAR VARIABLES

A. Z_{HH} (radar reflectivity factor)

Lightning flash rates were consistently highest in high reflectivity regions (> 55 dBZ) and spread throughout the area of reflectivity exceeding this threshold. In the development stage of the MCC, most lightning strikes occurred in a portion of the transition zone. The trailing stratiform region had low flash rates, and lightning there tended to occur in a region with relatively higher reflectivity (40–50 dBZ). In the mature stage, areas of high reflectivity (> 50 dBZ) decreased in size to the same magnitude as seen in the stratiform and trailing stratiform regions. Most of the convective region had reflectivity less than 55 dBZ (Fig. 4), but lightning flash rates remained very high within the convective region and portions of the transition zone. Lightning flash rates in the transition zone (Z_{HH} ~45 dBZ) started decreasing when the MCC transitioned from the development to mature stage. During the dissipating stage, total lightning decreased rapidly within the convective region, but the flash rate remained high in convective cores (Z_{HH} > 50 dBZ).

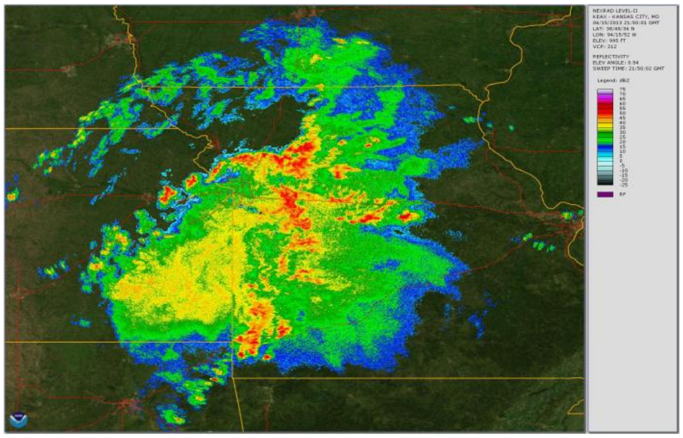

Figure 4. Z_{HH} during the mature stage of the MCC at 2150 UTC.

B. Z_{DR} *(differential reflectivity)*

Differential reflectivity (Z_{DR}) provides a measure of scatterer orientation, and in combination with other variables, a way to infer regions of liquid water and mixed-phase hydrometeors. Aggregated ice crystals typically have a Z_{DR} value less than or equal to zero. Columns and plates can have more positive values ranging from 2 to 4 dB. In addition, if a cloud contains a strong electric field, ice crystals tend to be vertically oriented, resulting in negative Z_{DR} values (Jacquelyn Ringhausen, personal communication 2014). The Z_{DR} is lower in ice particles with the same shape and orientation as raindrops, as the dielectric constant is much lower for ice. A decrease in Z_{DR} and collocated increase in Z_{HH} is often associated with large hailstones (e.g. Kumjian and Ryzhkov 2007).

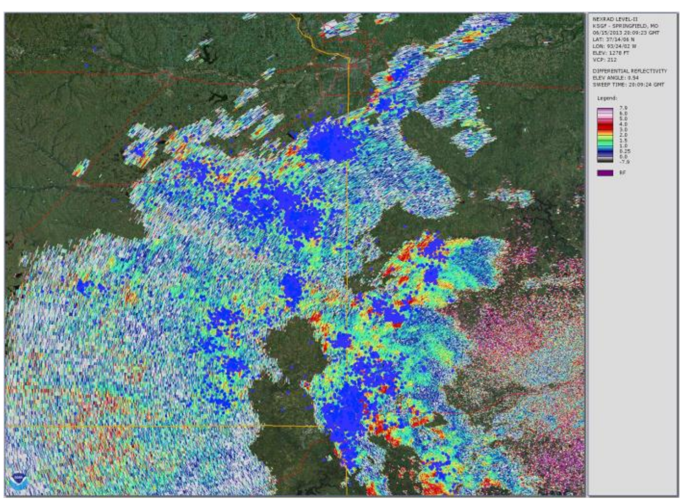

Figure 5. Z_{DR} in the development stage with overlaid lightning initiation points (blue dots) at 2009 UTC.

The IC flash rate was highest in areas with high differential reflectivity (> 4 dB), possibly due to strong updraft lifting supercooled water droplets above the melting level. The CG flash rate was highest along the boundary of highest Z_{DR} and Z_{HH}, apparently due to the mixed-phase area at the edge of updraft regions. Individual convective cells formed during the development stage of the MCC had high values of Z_{DR} in the convective region; regions of high lightning flash rate corresponded to a minimum threshold Z_{DR} value 1.5 dB (Fig. 5). As the MCC progressed through the mature stage (2149 UTC), Z_{DR} values decreased possibly due to weakening updraft leading to fewer ice crystals forming in convective updrafts. Lightning flashes remained in the region of Z_{DR} values between 1 and 2 dB. In the dissipating stage, Z_{DR} values increased where convective cells re-intensified. The transition zone had low Z_{DR} values and few lightning strikes. Z_{DR} was relatively noisy compared to Z_{HH}.

C. ρ_{hv} *(copolar correlation coefficient)*

Areas with high lightning flash rate were associated with ρ_{hv} values > 0.98, which is the region of graupel formation in the storm when collocated with Z_{DR} near zero and moderate Z_{HH} values (e.g. Kumjian et al. 2010). In some situations, large hailstones or rain mixed with hail will substantially reduce values of ρ_{hv}.

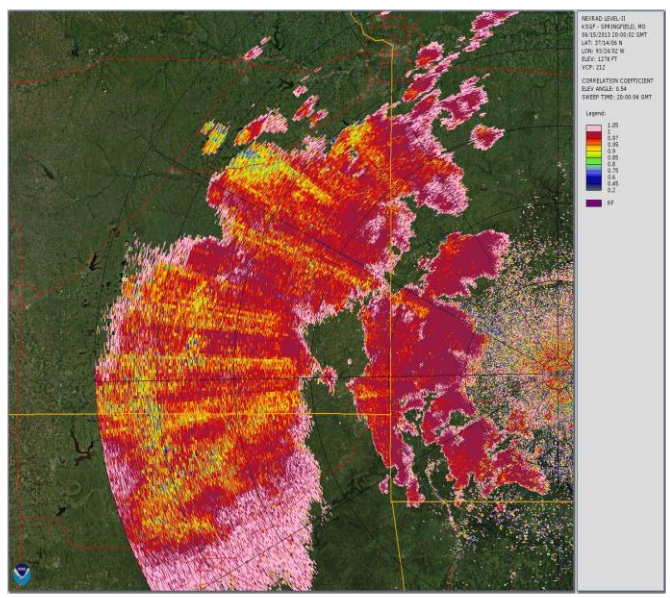

Figure 6. ρ_{hv} quality degradation downradial from convective cells at 2000 UTC.

The trailing stratiform region shows unrealistically low values of ρ_{hv} since the storm is far from the radar and subject to non-uniform beam filling (Fig. 6). ρ_{hv} values typically decrease with range since the sample volume has broadened and includes a greater diversity of hydrometeor species.

The ice and graupel layer in the trailing stratiform region is shallower, estimated between 3200 m and 5120 m, compared to the convective region where the ice and graupel layer is between 3200m and 9600 m. The smaller depth in the trailing stratiform region may indicate a lower flash rate since the total graupel mass is lower. In this MCC event, ρ_{hv} was not a good indicator of lightning flash rate far from the radar because convective cells near the radar caused significant noise farther away. The nearby strong convective regions cause non-uniform beam filling, resulting in significantly lower ρ_{hv} values over a large wedge (Warning Decision Training Branch, NOAA). Forecasters must account for data quality reductions of this variable far from the radar, especially downradial from convective cells.

D. K_{DP} (specific differential phase)

K_{DP} is used to estimate total liquid water content, and can help distinguish between liquid and frozen particles (e.g. Straka et al. 2000). The K_{DP} column often appears in strong updraft and can extend several kilometers above the melting level (Kumjian et al. 2007). Raindrops above the melting level in the K_{DP} column may indicate mixed supercooled water droplets and ice, which is favorable for lightning initiation.

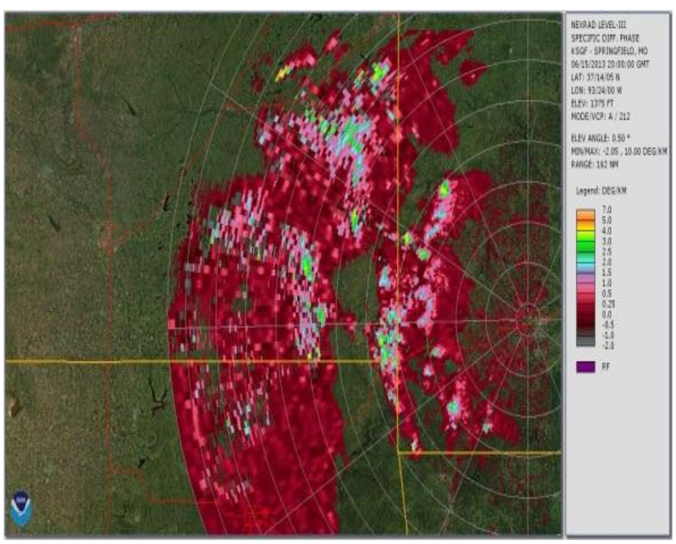

Figure 7. K_{DP} quality degradation due to non-uniform beam filling far from the radar and downradial from convective cells at 2000 UTC.

According to Loney et al. (2002) and Schlatter (2003), the K_{DP} column is associated with a high concentration of mixed-phase hydrometeors and is often collocated with high Z_{HH}. Lightning strikes were generally collocated with high K_{DP} (~2.5 deg km^{-1}), in deep convective updrafts. The trailing stratiform region had lower K_{DP} values (~0.25 deg km^{-1}) due to a lower concentration of liquid hydrometeors. (Fig. 8) K_{DP} values were high in the region generally associated with strong updraft, and the vertical K_{DP} column extended higher than in other regions. This was also the region with highest lightning flash rate. In the mature and dissipating stages, the K_{DP} distribution was similar to development stage in the convective region, with high K_{DP} values (~3 deg km^{-1}) generally associated with highest flash rates. The trailing stratiform region had K_{DP} values close to 1.5 deg km^{-1} at lowest elevation angle apparently due to melting hydrometeors. K_{DP}, like ρ_{hv}, has data quality issues far from the radar (Fig. 7). The main reason for this error is non-uniform beam filling. Nowcasters need to be cautious when using this polarimetric variable at long range.

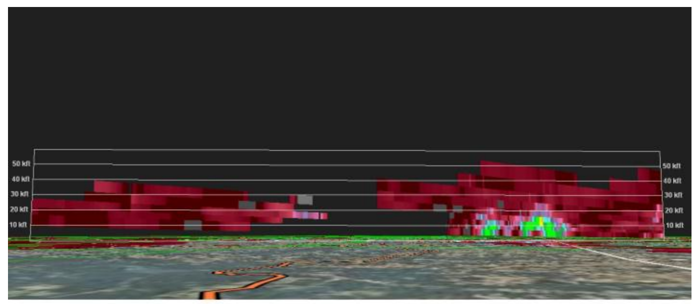

Figure 8. K_{DP} vertical cross-section at 2000 UTC.

V. VARIABLE LIGHTNING ACTIVITY IN ADJACENT CELLS

In our MCC, most lightning strikes were located in strong updraft regions. Palucki et al. (2011) point out that one difference between non-flash and flash-producing convective areas was the strength of the updraft and the breadth of the convection region, particularly at upper levels just prior to the flash. According to Bruning et al. (2006), the noninductive graupel-ice charging mechanism requires active riming supported by an updraft. They also note that hydrometeors in wet growth regions are less conducive to the rebounding collisions necessary for noninductive charge separation, which explained why regions of wet growth had smaller net charge density (Bruning et. al. 2006). The strong updraft also can loft liquid hydrometeors above the melting level to the mixed-phase region, where they become supercooled cloud water. Lightning flash rates in our MCC event support the conclusion of Bruning et al. (2006). Lightning strikes (CG and IC) were generally not initiated near the center of strong updrafts, which agrees with prior studies showing that a water coating discourages lightning initiation. Lightning strikes tend be focused in the mixed-phase region near the hail core.

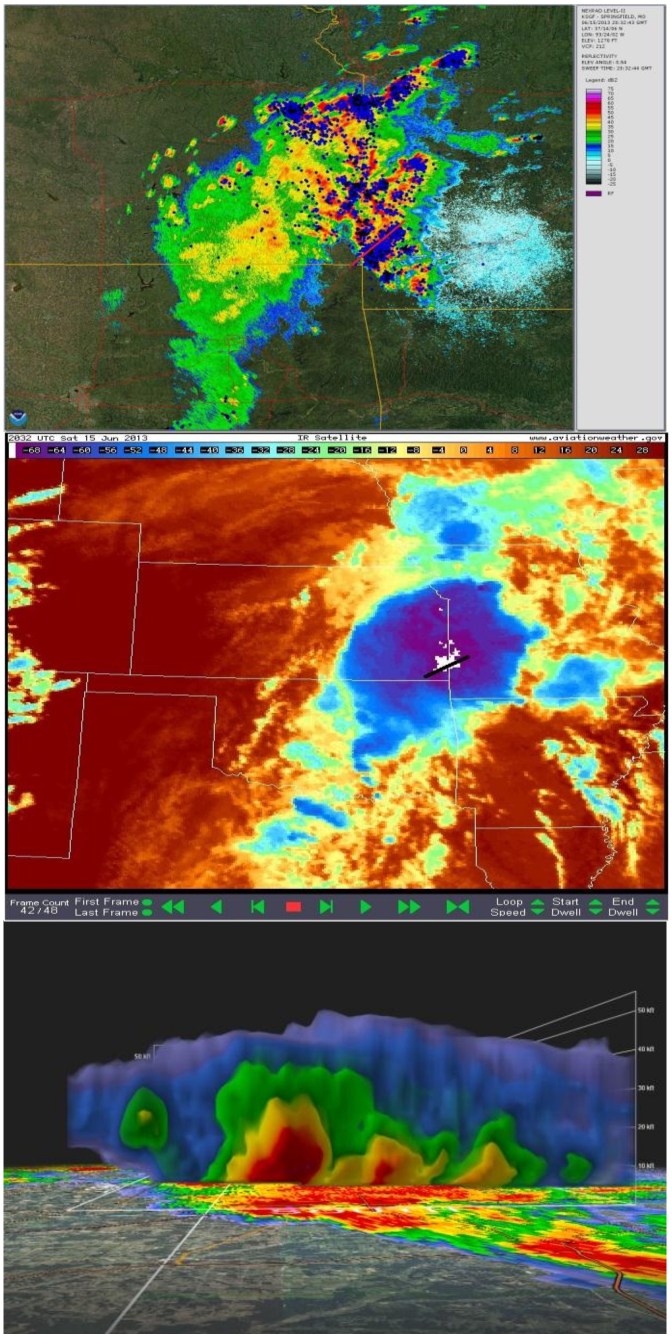

Figure 9.Comparsion of strikes (black dots = CG, blue dots = IC) (top), cross section in bottom panel shown as red line in top panel, cloud top temperature (middle), cross section shown as black line and vertical cross section (bottom), shown red at 2032 UTC.

Goodman et al. (1986) studied location of CG lightning in ten MCSs. Their results show that lightning strikes in these storms tend to occur in regions beneath cold cloud tops as depicted by infrared satellite imagery. This corresponds to our analysis, in which we found the most lightning strikes in the region with coldest cloud tops. The strikes were focused in the region with temperature lower than -52°C as estimated by an infrared satellite image during the development stage. During the mature and dissipating stages, estimated temperature in the convective area's top was not as low as in the development stage, but highest lightning flash rate was still collocated with coldest cloud tops (Fig. 9).

The strong updraft may also result in a deeper mixed-phase hydrometeor layer around the updraft core, causing intense lightning flash rates. Moving away from the center of a strong updraft, the mixed-phase layer becomes shallower and the vertical component of the wind decreases. There is mesoscale upward motion in the stratiform cloud and mesoscale subsidence between the base of the stratiform cloud and the surface (e.g. Biggerstaff and Houze 1993). Hence, the vertical column immediately behind the convective cells is characterized by a large vertical shear in the horizontal flow. They also suggest that front-to-rear flow was responsible for spreading the ice particles, which were produced in the convective cells, rearward into the transition zone and trailing stratiform region. This may explain why some lightning flashes occurred outside the convective region (Fig.10). Rutledge et al. (1987) indicated that the stratiform region has a very small amount of cloud water, so riming is of lesser importance. This agrees with our results, since low K_{DP} values were present in this region. The trailing stratiform region has only weak updraft areas, and thus is less favorable for initiation of lightning strikes. Some areas near the edge of the MCC have high reflectivity, but no CG and IC strikes possibly due to these cells being young, resulting in less-mature hydrometeor distributions compared to the earlier cells which contained higher flash rates.

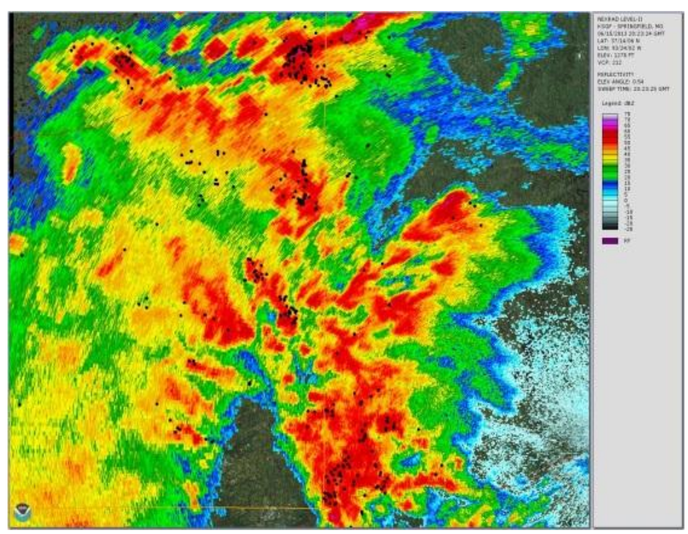

Figure 10. CG lightning activity occurrence around high-reflectivity regions at 2023UTC

We hypothesize that strikes in the northeast portion of the convective region were related to the anvil location. The anvil primary consists of ice particles, but the layer is very thin compare to the other part of the storm. The vertical distance between the anvil and ground is large, so this region is more favorable to high-amperage CG lightning strikes which extend from the anvil to the surface as we observed (Fig. 11).

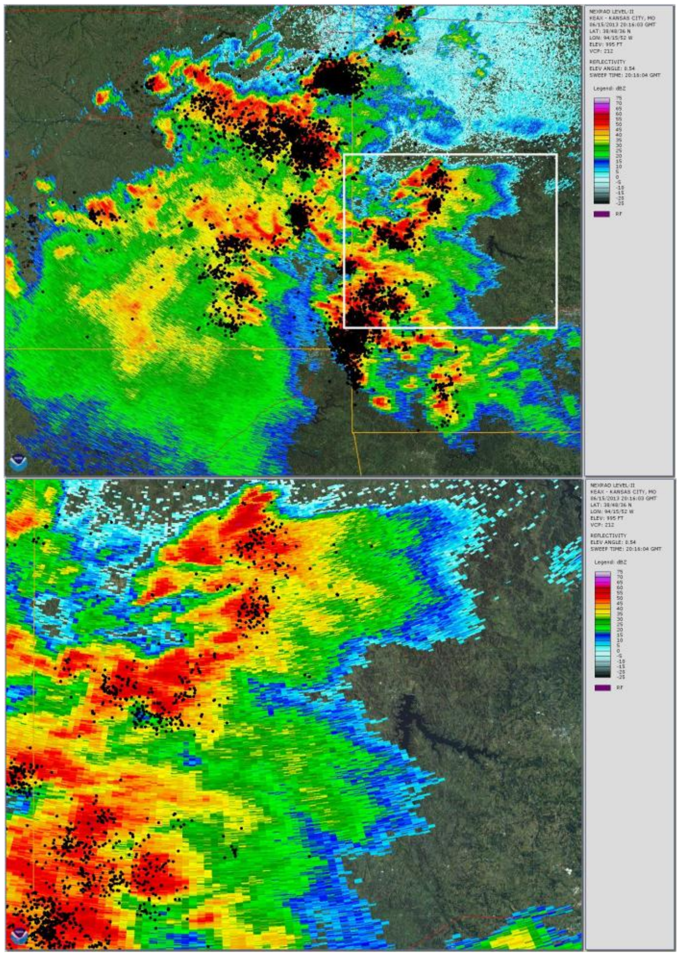

Figure 11. CG lightning occurrence under the anvil region (bottom) at 2016 UTC.

VI. CONCLUSION AND FUTURE RESEARCH

A study has been undertaken to examine the evolution of lightning in an MCC compared to polarimetric radar variables, and to infer microphysics favorable for charge separation. In the June 15-16, 2013, MCC event, IC was collocated with high Z_{HH} and Z_{DR} through the entire life cycle of the MCC. CG flash rate was only one-tenth of the IC rate, and tended to cluster around the edge of the region of high Z_{HH}. Using ρ_{hv} may be especially effective for identification of graupel and mixed-phase hydrometeors, but must be interpreted with caution, especially far from the radar. K_{DP} can indicate where liquid may be present, possibly helping aircraft avoid the region, but it has same range quality degradation as ρ_{hv}. As prior studies have shown, MCCs in the North America may exhibit strongly-varying electrical activity from case to case, depending on the local environment. Additional research should focus on polarimetric radar variable differences between positive/negative flashes and flashes with variable peak intensity.

Acknowledgments. We wish to thank Earth Networks-WeatherBug for access to the lightning data used in this study. The research reported here was partially support by the University of Nebraska-Lincoln under the Undergraduate Creative Activities and Research Experiences program (UCARE).

REFERENCES

Biggerstaff, Michael I., Robert A. Houze, 1993: Kinematics and Microphysics of the Transition Zone of the 10–11 June 1985 Squall Line. *J. Atmos. Sci.*, **50**, 3091–3110.

Bruning, Eric C., W. David Rust, Terry J. Schuur, Donald R. MacGorman, Paul R. Krehbiel, William Rison, 2007: Electrical and Polarimetric Radar Observations of a Multicell Storm in TELEX. *Mon. Wea. Rev.*, **135**, 2525–2544.

Goodman, S. J., D. R. MacGorman, 1986: Cloud-to-Ground Lightning Activity in Mesoscale Convective Complexes. *Mon. Wea. Rev.*, **114**, 2320–2328.

Hunter, Steven M., Terry J. Schuur, Thomas C. Mapshall, W. David Rust, 1992: Electric and Kinematic Structure of the Oklahoma Mesoscale Convective System of 7 June 1989. *Mon. Wea. Rev.*, **120**, 2226–2239.

Kumjian, Matthew R., Alexander V. Ryzhkov, 2008: Polarimetric Signatures in Supercell Thunderstorms. *J. Appl. Meteor. Climatol.*, **47**, 1940–1961

Kumjian, Matthew R., Alexander V. Ryzhkov, 2010: The Impact of Evaporation on Polarimetric Characteristics of Rain: Theoretical Model and Practical Implications. *J. Appl. Meteor. Climatol.*, **49**, 1247–1267.

Loney, Matthew L., Dušan S. Zrnić, Jerry M. Straka, Alexander V. Ryzhkov, 2002: Enhanced Polarimetric Radar Signatures above the Melting Level in a Supercell Storm. *J. Appl. Meteor.*, **41**, 1179–1194.

Maddox, Robert A., 1980: Meoscale Convective Complexes. *Bull. Amer. Meteor. Soc.*, **61**, 1374–1387.

Mapes, Brain E., Robert A. Houze, 1993: Cloud Clusters and Superclusters over the Oceanic Warm Pool. *Mon. Wea. Rev.*, **121**, 1398–1416.

Makowski, Jeffrey A., Donald R. MacGorman, Michael I. Biggerstaff, William H. Beasley, 2013: Total Lightning Characteristics Relative to Radar and Satellite Observations of Oklahoma Mesoscale Convective Systems. *Mon. Wea. Rev.*, **141**, 1593–1611.

Mohr, Karen I., Edward J. Zipser, 1996: Mesoscale Convective Systems Defined by Their 85-GHz Ice Scattering Signature: Size and Intensity Comparison over Tropical Oceans and Continents. *Mon. Wea. Rev.*, **124**, 2417–2437.

Palucki, Jennifer L., Michael I. Biggerstaff, Donald R. MacGorman, Terry Schuur, 2011: Comparison between Low-Flash and Non-Lightning-Producing Convective Areas within a Mature Mesoscale Convective System. *Wea. Forecasting*, **26**, 468–486.

Ringhausen, Jacquelyn, 2014: Getting to know Dual-Pol: A Case Study Comparison of C-Band and S-Band Dual-Polarization Radars in Northern Alabama, NOAA, Hardin, IL

Ringhausen, Jacquelyn, personal communication, February 11 2014

Rutledge, Steven A., Donald R. MacGorman, 1988: Cloud-to-Ground Lightning Activity in the 10–11 June 1985 Mesoscale Convective

System Observed during the Oklahoma–Kansas PRE-STORM Project. *Mon. Wea. Rev.*, **116**, 1393–1408.

Schlatter, P. T., 2003: Polarimetric radar and in-situ measurements of a nontornadic supercell. M.S. thesis, School of Meteorology, University of Oklahoma, 97 pp.

Straka, Jerry M., Dusan S. Zrnić, Alexander V. Ryzhkov, 2000: Bulk Hydrometeor Classification and Quantification Using Polarimetric Radar Data: Synthesis of Relations. *J. Appl. Meteor.*, **39**, 1341–1372.

Parker, Matthew D., Richard H. Johnson, 2000: Organizational Modes of Midlatitude Mesoscale Convective Systems. *Mon. Wea. Rev.*, **128**, 3413–3436.

Dual-Polarization Radar Principles and system Operations,Warning Decision Training Branch, NOAA http://www.wdtb.noaa.gov/courses/dualpol/documents/DualPolRadarPrinciples.pdf